Journal Name

COMMUNICATION

Connection of zinc paddle-wheels in a pto-type metal-organic framework with 2-methylimidazolate and subsequent incorporation of charged organic guests

NakeunKo,[a] KyungkyouNoh,[a] Siyoung Sung,[a] HyeJeong Park,[*a] SangYoun Park[*b] and Jaheon Kim[*a]

A microporous metal-organic framework (mIm-MOF-14) has doubly interpenetrated anionic frameworks resulting from 2-methylimidazolate linking Zn(II) paddle-wheels of charge-neutral pto-type networks, and allows the inclusion of tetramethylammonium ion to exert an enhanced CO_2 affinity.

Metal-organic frameworks (MOFs) are porous crystalline solids prepared through solvothermal reactions between metal ions and bridging ligands. Under proper reaction conditions, a series of isoreticular structures have been prepared simply by changing ligands as exemplified in isoreticular MOFs(IRMOFs) exhibiting primitive cubic net (**pcu**),[1] or (3,4)-connected net (**tbo** or **pto**).[2] This reticular chemistry is very effective for controlling pore environments, which are directly influential in applications. This synthetic strategy is reinforced by utilizing default structures and their relationship as demonstrated in the preparation of FJI-1[3] and DUT-23(M)[4] (M=Zn, Co, Cu, and Ni divalent ions). These MOFs are composed of M_2 paddle-wheels connected by two kinds of organic linkers, benzene-1,3,5-tribenzoate (BTB) and 4,4'-bpyto afford a general formula of $M_3(BTB)_2(4,4'-bpy)_{1.5}$. The framework connectivity of FJI-1[3] and DUT-23(M)[4] is described as **ith-d** net which is also achieved in DTU-6[5] or MOF-205[6] with different inorganic clusters (Zn_4O units) and different combination of the organic linkers (BTB and naphthalene-2,6-dicarboxylate (NDC)). It is noteworthy that FJI-1 and DUT-23(M) have a topological relationship with a **pto**-type MOF-143 formulated as $Cu_3(BTB)_2$ without coordinated H_2O molecules (Fig. 1).[7] As their formula imply, the insertion of 4,4'-bpy bridging ligands between M_2 paddle-wheels in a $M_3(BTB)_2$ **pto** structure resulted in the **ith-d** type networks.[3,4] Here, we report that anionic 2-methylimidazolates (mIm) can be also placed between Zn_2 paddle-wheels in a **pto** type framework, leading to doubly interpenetrated anionic

frameworks unlike FJI-1 and

Fig. 1 Comparison of the simplified crystal structures of MOF-143, MOF-14, FJI-1 or DUT-23, and Ni-MOF. BTB linkers are displayed with three-connecting lines and M_2 paddle-wheels are with polyhedrons. Red lines represent the 4,4'-bpybridging ligands in FJI-1 or DUT-23. The **a** and **b** values in the figures and inset table are M···M distances. Both MOF-14 and Ni-MOF are doubly interpenetrated structures and their single frameworks are shown for simplicity.

	MOF-143	MOF-14	FJI-1 (DUT-23)	Ni-MOF
a(Å)	11.10	14.00	11.02	14.93
b(Å)	11.10	7.66	11.02	6.19

DUT-23(M) MOFs. The incorporation of tetramethylammonium (TMA) ion to the anionic MOF increases the isosteric heat of CO_2 adsorption.

Bridging pyridyl ligands can be also incorporated in MOFs not from the start but also in a post-modification manner.[8] Regardless of the procedures, the insertion of additional spacers in a parent framework needs the consideration on geometric

factors along with the topological relationship between the MOFs. In the case of FJI-1 or DUT-23, the distance of 11.02 Å between the two metal ions in paddle-wheels connected by the 4,4'-bpy spacer is well-matched to the M…M separation of 11.10 Å in MOF-143 (Fig. 1a).[7] This means that the coordination of 4,4'-bpy (7.0 Å in its length) through its terminal N atoms to the metal centres in paddle-wheels does not produce the severe structural distortion in the **pto** structure. However, this similar situation is not expected for a much shorter linker such as 2-methylimidazolate which has an N…N distance of 2.1 Å. Fortunately other parent MOFs can accommodate such a short spacer. That is, unlike MOF-143, MOF-14 has unconnected Cu paddle-wheels with small (7.66 Å) and large (14.00 Å) M…M separations in doubly interpenetrated frameworks (Fig. 1b).[9] Similarly to MOF-14, a 'Ni-MOF', $[Ni_3(BTB)_2(H-mIm)_{1.5}(H_2O)_{1.5}]$, where 2-methylimidazole (H-mIm) is just coordinated to Ni ions, showed two 14.93 and 6.19 Å M…M distances (Fig. 1d).[10] Particularly, the short separation (6.19 Å) in Ni-MOF matches the sum of bridging mIm (2.1 Å) and two M-N coordination bonds (2×2.0 Å). Indeed, the next step is to find a pertinent reaction condition for successful incorporation of mIm into a **pto**-type MOF.

When a solvothermal reaction of $Zn(NO_3)_2 \cdot 6H_2O$ (510 mg) and H_3BTB (192 mg) in *N,N*-dimethylformamide (DMF; 30.0 mL) with 2-methylimidazole (H-mIm; 160 mg) was carried out at 95 °C for 2 days, light-yellow block crystals (197 mg) were obtained as a product (hereafter mIm-MOF-14).† This reaction condition does not involve zeolitic-imidazolate frameworks (ZIFs) as by-products can be prepared from Zn(II) and imidazole. The bulk phase purity was confirmed by the comparison of the measured and simulated powder X-ray diffraction (PXRD) patterns (Fig. S1).

While the MOF structures comprising of M_2 paddle-wheels and three-connecting linkers are likely to have **tbo** or **pto** topology,[7] the combination of BTB and M_2 paddle-wheels has exclusively produced **pto** frameworks. Single-crystal X-ray diffraction analysis reveals that two independent **pto** type $Zn_3(BTB)_2$ frameworks are mutually interpenetrated (Fig. 2).
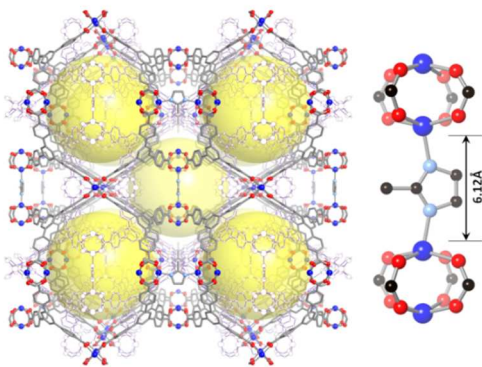
Fig. 2 The Crystal structure of mIm-MOF-14. One of the interpenetrated frameworks is displayed with light purple sticks. Coordinated H-mIm molecules are not shown. Large yellow spheres represent the 16 Å

pores with considering van der Waals contacts. An ordered model of the bridging mIm is also shown with a Zn…Zn distance. Colour codes: C, black; N, sky blue; O, red; Zn, blue.
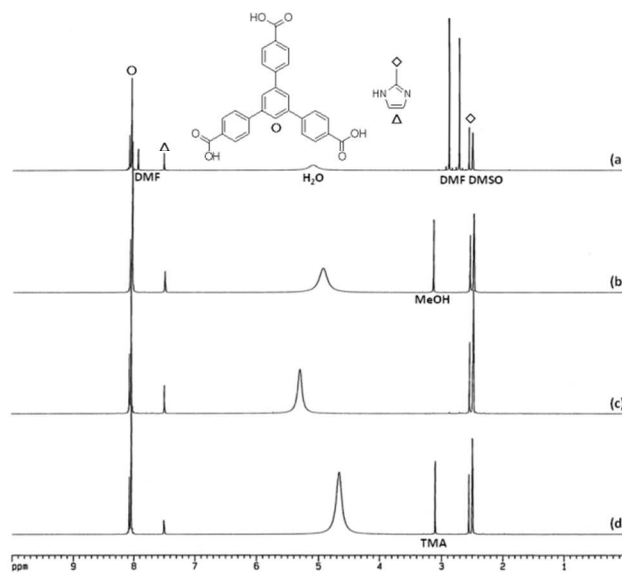
Fig. 3 ^{1}H-NMR spectra of digested samples in DCl/DMSO-d_6: (a) as-prepared mIm-MOF-14, (b) MeOH-exchanged mIm-MOF-14, (c) activated mIm-MOF-14, and (d) activated TMA@mIm-MOF-14. The TMA signal in (d) is observed at 3.10 ppm while the MeOH signal in (b) at 3.15 ppm. The BTB protons (○) are collectively shown at 8.1 ppm. (See Figures S3-S8 in ESI for details).

There are two kinds of mIm in an asymmetric unit (Fig. S2); one coordinated to Zn1 is bridging two Zn paddle-wheels, and the other is just coordinated to Zn ions (Zn2). Similarly to MOF-14 and Ni-MOF mentioned above, mIm-MOF-14 has short and long M…M separations (**a** and **b** in Fig. 1). mIm ligands connect Zn paddle-wheels with the separation of 6.12 Å (Fig. 2) without disturbing the $Zn_3(BTB)_2$ framework structure, but the large separation (14.49 Å) is too long to link. Assuming that the bridging mIm is an imidazolate and the dangling mIm is an imidazole form, the framework formula was tentatively supposed to be $[(guest)^+]_{4/3}[Zn_3(BTB)_2(mIm)_{3/4}(H-mIm)_{6/4}]$.

A certain guest carrying a positive charge is necessary for making a charge balance in the proposed formula. A possible candidate may be a solvated Zn(II) ion or a *N,N*-dimethylammonium ion in the pores which is sometimes produced from the decomposition of solvent DMF.[11] Since the guests could not be identified in single-crystal X-ray structure due to the severe disorder, we conducted elemental analyses (EA) and thermogravimetric analyses (TGA). However, EA and TGA data excluded the presence of charged guest molecules in the pores. ^{1}H-NMR measurements on the digested samples of as-prepared, solvent-exchanged, and activated mIm-MOF-14 gave only the signals from H_3BTB, H-mIm, and occluded solvent molecules (Fig. 3). In particular, the signal integration ratio between H_3BTB and H-mIm for an activated sample was closed to 2 : (9/4) (Fig. S7). As a result, the chemical formula for mIm-MOF-14 has been suggested as $(H_2\text{-}mIm^+)_{3/4}[Zn_3(BTB)_2(mIm)_{3/4}(H\text{-}mIm)_{3/4}]$ ($H_2\text{-}mIm^+$ =

protonated 2-methylimidazole); an anionic mIm links two Zn centres, and only a half of coordinated H-mIm is protonated. Hydronium ion as counter ion has not been considered because it is seldom observed in MOFs.

As expected, mIm-MOF-14 shows the same pto-type $M_3(BTB)_2$ three-dimensional structures as in MOF-14 or Ni-MOF. Considering the Zn…Zn distances of a = 6.12 Å and b = 14.49 Å, mIm-MOF-14 resembles Ni-MOF-14 more than MOF-14. While FJI-1 and DUT-23 linked by 4,4'-bpy are non-interpenetrated, mIm-MOF-14 is doubly interpenetrated because the unconnected Zn_2 paddle-wheels allow the penetration of a second framework. The 16 Å pores in mIm-MOF-14 provide a void space of 49.7 % per a unit cell as calculated by PLATON.[12] In spite of the structural similarity, mIm-MOF-14 has a more stable framework than Ni-MOF. While Ni-MOF showed a structural transformation when activated at 100°C, the PXRD pattern of as-prepared sample for mIm-MOF-14 was retained after the activation (Fig. S1).

Ni-MOF does not uptake N_2 gas and only permits the adsorption of smaller gases such as H_2O, CO_2, and H_2 due to its small openings.[10,13] Thus, the evacuation of mIm-MOF-14 was also concerned. In fact, the TGA trace of as-prepared mIm-MOF-14 shows that the occluded ca. 7.3 DMFs (calcd. 29.9%) are removed at a relatively high temperature of 230°C with a weight loss of 31% (Fig. S9). In addition, the solvent exchange has not been easily performed with common methods. The occluded DMFs could be replaced with THF by refluxing the as-prepared mIm-MOF-14 in THF for 48 h as confirmed by ^{1}H-NMR analyses (Fig. S4). When MeOH was used instead of THF, it took only 1 day for the completion of the guest exchange (Fig. S5). When the MeOH-exchanged mIm-MOF-14 was activated at 80 °C for 10 h under dynamic vacuum, the guest molecules were completely removed (Fig. S6 and S10). A nitrogen sorption measurement at 77 K (Fig. 4a) resulted in the Brunauer–Emmett–Teller (BET) and Langmuir surface areas of 1011 and 1507 m^2/g, respectively. The surface area of mIm-MOF-14 is comparable to that (Langmuir, 1502 m^2/g) of MOF-14, but much smaller than the BET surface areas of FJI-1 (Zn; 4043 m^2/g)[3] and DUT-23 (Ni; 5590 m^2/g).[14]

We admit that the identification of the cationic species in mIm-MOF-14 is arguable. However, it is presumed that a cation exchange would happen if there is an exchangeable cationic species in the framework. The cation exchange with (N,N-dimethyl)HCl in MeOH made the mIm-MOF-14 almost amorphous, which is ascribed to the generation of HCl. Therefore, a neutral salt, TMA chloride was selected as the source of a cationic organic guest. To a MeOH solution of [TMA]Cl(0.1M, 100 mL), as-synthesized mIm-MOF-14 (300 mg) was refluxed for 48 h. The collected crystals were rinsed with fresh MeOH (30 mL × 5) and activated at 80 °C for 10 h. ^{1}H-NMR spectra on the digested samples show that the signal integration ratio between H_3BTB and all the imidazole molecules was still 2 : (9/4) and TMA was included as many as 0.75 based on $[Zn_3(BTB)_2]$ (Fig. S7). This indicates that the protonated 2-methylimidazole in mIm-MOF-14 was deprotonated during the incorporation of TMA in the pores.

The chemical composition was assigned as $(TMA^+)_{3/4}[Zn_3(BTB)_2(mIm)_{3/4}(H\text{-}mIm)_{3/2}]$ (TMA@mIm-MOF-14) based on the EA, TGA, and ^{1}H-NMR measurements. After the full incorporation of TMA, the surface areas decreased to 653 m^2/g (BET) and 858 m^2/g (Langmuir) (Fig. 4a). The activated TMA@mIm-MOF-14 (48 h) showed the same PXRD pattern as those of both as-prepared and activated mIm-MOF-14 (Fig. S1), suggesting that the framework structure was retained during the TMA inclusion process.
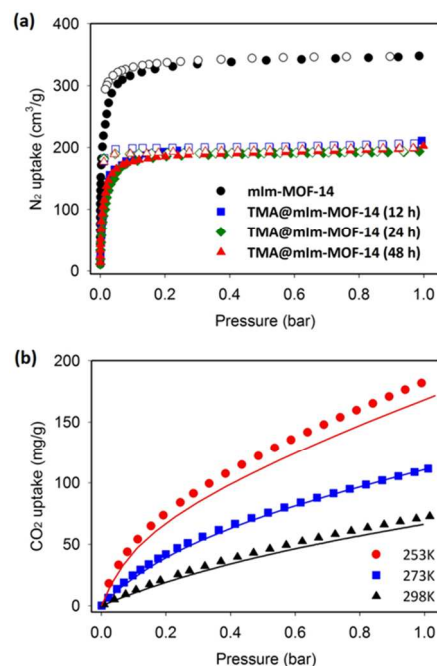
Fig. 4 (a) N_2 sorption isotherms of mImMOF-14 (circles) and TMA@mIm-MOF-14s (12h, squares; 24h, diamonds; 48h, triangles) measured at 77K. Filled shapes: adsorption. Open shapes: desorption. (b) CO_2 sorption isotherms of mIm-MOF-14 (lines) and TMA@mIm-MOF-14 (48 h) (marks) measured at 253 (circles), 273 (squares), and 298 K (triangles), respectively.

In order to understand the guest incorporation property of mIm-MOF-14, we also prepared two samples containing partially incorporated TMA by refluxing as-synthesized mIm-MOF-14 respectively for 12 and 24 h. Similarly to the TMA@mIm-MOF-14 (48 h), the TMA contents were determined by the integration of the ^{1}H-NMR signals. The analyses indicated that ca. 53 and 72% of TMA were incorporated in mIm-MOF-14 after 12 and 24 h, respectively (Fig. S7 and S8). The partial exchange of the cationic species suggested the gradual decrease in the surface areas for the TMA@mIm-MOF14 (12 h, 24 h) samples. Contrary to this expectation and curiously, they showed almost same N_2 sorption isotherms as that of the TMA@mIm-MOF-14 (48 h). As a repeated TMA inclusion experiment gave the same result, it is presumed that mIm-MOF-14 might have a peculiar guest-exchange property although we are not able to present reasonable evidence. Nevertheless, the CO_2 sorption property

of the TMA-included sample was further investigated using the TMA@mIm-MOF-14 (48 h).

The amount of CO_2 uptake in mIm-MOF-14 is moderate (Fig. 4b) and the heat of CO_2 adsorption at zero coverage is 24 kJ/mol (Fig. S13) which is within the reported values of MOFs (15 ~ 63 kJ/mol).[13a] Considering that the –NH functionality in organic linkers can contribute positively to the CO_2 affinity,[15] the relatively low CO_2 affinity of mIm-MOF-14 may be ascribed to the steric congestion produced by 2-methyl group in H-mIm. Interestingly, although the surface area has been reduced, TMA@mIm-MOF-14 shows the enhanced CO_2 affinity; it adsorbs almost same amounts of CO_2 as those of mIm-MOF-14 at all the measured temperatures, and has an increased heat of CO_2 adsorption to 25 kJ/mol (Fig. S15). This result is in accordance with the improved CO_2 adsorption behaviours shown in the cation-exchanged bio-MOF-1,[16] and supports the successful inclusion of TMA.

As demonstrated in some 'mixed-ligand MOFs' such as UMCM-1[17] (2 different carboxylates), MUF-7[18](3 different carboxylates), Bio-MOF-100[19] (carboxylate and adeninate), and MAC-6[20] (carboxylate and triazolate), there is a high possibility of achieving new types of MOFs with mixed ligands. In this regard, the present work illustrates a plausible way to make a 'mixed-ligand' MOF by utilizing both geometric and topological properties of pto-type MOFs. The unique aspect for the resulting MOF (mIm-MOF-14) is that, unlike FJI-1 and DUT-23(M), anionic 2-methylimidazolate is inserted into the $M_3(BTB)_2$ frameworks to give essentially a negative-charged framework, thus admitting the impregnation of positive-charged guests.

Notes and references

[a]Institute for Integrative Basic Sciences, Department of Chemistry, Soongsil University, Seoul 156-743, Republic of Korea. Fax: +82-2-824-4383; Tel: +82-2-820-0459; E-mail: parkhyejeong83@gmail.com (H.J.P.), jaheon@ssu.ac.kr(J.K.).
[b]School of Systems Biomedical Science, Soongsil University, Seoul 156-743, Republic of Korea. Fax: +82-2-824-4383; Tel: +82-2-820-0459; E-mail: psy@ssu.ac.kr.

† Electronic Supplementary Information (ESI) available: general experimnetal procedures, materials syntheses, X-ray crystallographic data, PXRD patterns, ^{1}H-NMR spectra, TGA thermograms, and plots for isosteric heats of CO_2 adsorption. CCDC-987525 for mIm-MOF-14.See DOI: 10.1039/c000000x/

1   (a) H. Li, M. Eddaoudi, M. O'Keeffe and O. M. Yaghi, *Nature*, 1999, **402**, 276; (b) M. Eddaoudi, J. Kim, N. L. Rosi, D. T. Vodak, J. Wachter, M. O'Keeffe and O. M. Yaghi, *Science*, 2002, **295**, 469.
2   (a) S. S. Y. Chui, S. M. F. Lo, J. P. H. Charmant, A. G. Orpen and I. D. Williams, *Science*, 1999, **283**, 1148; (b) D. Sun, S. Ma, Y. Ke, D. J. Collins and H.-C. Zhou, *J. Am. Chem. Soc.*, 2006, **128**, 3896; (c) S. Ma, D. Sun, M. Ambrogio, J. A. Fillinger, S. Parkin and H.-C. Zhou, J. *Am. Chem. Soc.*, 2007, **129**, 1858.
3   D. Han, F.-L. Jiang, M.-Y. Wu, L. Chen, Q.-H. Chena and M.-C. Hong, *Chem. Commun.*, 2011, **47**, 9861.
4   N. Klein, I. Senkovska, I. A. Baburin, R. Grnker, U. Stoeck, M. Schlichtenmayer, B. Streppel, U. Mueller, S. Leoni, M. Hirscher and S. Kaskel, *Chem. Eur. J.*, 2011, **17**, 13007.
5   N. Klein, I. Senkovska, K. Gedrich, U. Stoeck, A. Henschel, U. Mueller and S. Kaskel, *Angew. Chem. Int. Ed.*, 2009, **48**, 9954.
6   H. Furukawa, N. Ko, Y. B. Go, N. Aratani, S. B. Choi, E. Choi, A. O. Yazaydin, R. Q. Snurr, M. O'Keeffe, J. Kim and O. M. Yaghi, *Science*, 2010, **329**, 424.
7   H. Furukawa, Y. B. Go, N. Ko, Y. K. Park, F. J. Uribe-Romo, J. Kim, M. O'Keeffe and O. M. Yaghi, *Inorg. Chem.*, 2011, **50**, 9147.
8   (a) H. J. Park and M. P. Suh, *Chem. Eur. J.*, 2008, **14**, 8812; (b) B. J. Burnett, P. M. Barron, C. Huand and W. Choe, *J. Am. Chem. Soc.*, 2011, **133**, 9984; (c) S. Jeong, D. Kim, X. Song, M. Choi, N. Park and M. S. Lah, *Chem. Mater.*, 2013, **25**, 1047.
9   B. Chen, M. Eddaoudi, S. T. Hyde, M. O'Keeffe and O. M. Yaghi, *Science*, 2001, **291**, 1021.
10 P. Maniam and N. Stock, *Inorg. Chem.*, 2011, **50**, 5085.
11 A. D. Burrows, K. Cassar, R. M. W. Friend, M. F. Mahon, S. P. Rigby and J. E. Warren, *CrystEngComm*, 2005, **7**, 548.
12 A. L. Spek, PLATON, A Multipurpose Crystallographic Tool; Utrecht University: Utrecht, The Netherlands, 2011
13 (a) K. D. Sumida, L. Rogow, J. A. Mason, T. M. McDonald, E. D. Bloch, Z. R. Herm, T. H. Bae and J. R. Long, *Chem. Rev.*, 2012, **112**, 724; (b) D. R. Lide, CRC Handbook of Chemistry and Physics; CRC Press: Boca Raton, FL, 2004.
14 X. Song, T. K. Kim, H. Kim, D. Kim, S. Jeong, H. R. Moon and M. S. Lah, *Chem. Mater.*, 2012, **24**, 3065.
15 (a) J. An, S. J. Geib and N. L. Rosi, *J. Am. Chem. Soc.*, 2010, **132**, 38; (b) F. Debatin, A. Thomas, A. Kelling, N. Hedin, Z. Bacsik, I. Senkovska, S. Kaskel, M. Junginger, H. Mller, U. Schilde, C. Jäger, A. Friedrich and H.-J. Holdt, *Angew. Chem. Int. Ed.*, 2010, **49**, 1258; (c) E. Barea, G. Tagliabue, W.-G. Wang, M. Pérez-Mendoza, L. Mendez-Liñan, F. J. López-Garzon, S. Galli, N. Masciocchi and J. A. R. Navarro, *Chem. Eur. J.*, 2010, **16**, 931.
16 J. An and N. L. Rosi, *J. Am. Chem. Soc.*, 2010, **132**, 5578.
17 (a) K. Koh, A. G. Wong-Foy and A. J. Matzger, *Angew. Chem. Int. Ed.*, 2008, **47**, 677; (b) K. Koh, A. G.Wong-Foy and A. J. Matzger, *J. Am. Chem. Soc.*, 2010, **132**, 15005.
18 L. Liu, K. Konstas, M. R. Hill and S. G. Telfer, *J. Am. Chem. Soc.*, 2013, **135**, 17731.
19 J. An, O. K. Farha, J. T. Hupp, E. Pohl, J. L. Yeh and N. L.Rosi, *Nat. Commun.*, 2012, **3**, 604.
20 F. Yang, Q. Zheng, Z. Chen, Y. Ling, X. Liu, L. Weng and Y. Zhou, *CrystEngComm*, 2013, **15**, 7031.